P11B.5

ACCURACY OF ZDR DATA AND IMPLICATIONS TO OPERATIONAL RADAR MEASUREMENTS

Ronald Hannesen*, Jörg Borgmann, Peter Gölz, and Frank Gekat
Selex-Gematronik, Neuss, Germany

1. INTRODUCTION

Measurements of differential reflectivity (ZDR) of precipitation need to be observed with an accuracy of 0.1 to 0.2 dB to be operationally usable e.g. for precipitation classification or for dual-polarisation rain rate algorithms (e.g. Melnikov et al., 2003). Unfortunately, measurements of ZDR may be biased due to several reasons. A general system offset can be corrected for by observations of stratiform rain with a vertically pointing antenna (e.g. Gourley et al, 2006). Methods exist to correct for differential attenuation from rain (e.g. Bringi et al., 2001). Obstacles near to the radar may cause a significant systematic bias, which is depending on the azimuth angle (e.g. Gourley et al, 2006). Also, ZDR bias from partial beam blockage has been reported (e.g. Giangrande and Ryzhkov, 2005).

For this study, two possible sources of ZDR bias and their implication to operational radar measurements are investigated:

- The dependence of ZDR measurements on the azimuth angle, for an obstacle-free radar without radome
- The effect of partial beam blockage on ZDR measurements.

2. AZIMUTHAL VARIATION OF ZDR

To avoid a systematic azimuth angle dependent bias of ZDR, obstacles near the radar should be removed as far as possible. Furthermore, a properly designed radome should be used, e.g. a random-panel radome instead of an "orange peel" radome (Manz et al., 1998). It is also important that the rotary joints cause no angle-dependent bias.

To investigate the systematic azimuth angle dependency of ZDR, a C-band radar without radome has been installed at the Selex-Gematronik factory. Two different measurement methods were performed:

- ZDR measurement of the hardware using a test signal generator
- Long-time PPI measurements of stratiform precipitation at different elevation angles

2.1 Measurements with a Test Signal Generator

The accuracy of the rotary joints (more precisely: the maximum variation of the insertion loss difference with respect to the rotation angle of the rotary joint) is specified to be better than 0.1 dB. To investigate the ZDR variability in a real system, a test signal generator (TSG) was mounted in the elevation box of the antenna pedestal. A cw test signal was split by a power divider and fed into the horizontal and vertical wave guide system. This test signal run through the azimuth rotary joints into the radar receiver. ZDR data versus azimuth were averaged over 10 full turns with a resolution of 1°.

A result is shown in Fig. 1. There, the TSG measurements have been multiplied with a factor of two to care for two-way analyses. The phase of a first-order Fourier fit is 140 deg, and the variability is 0.044 dB.

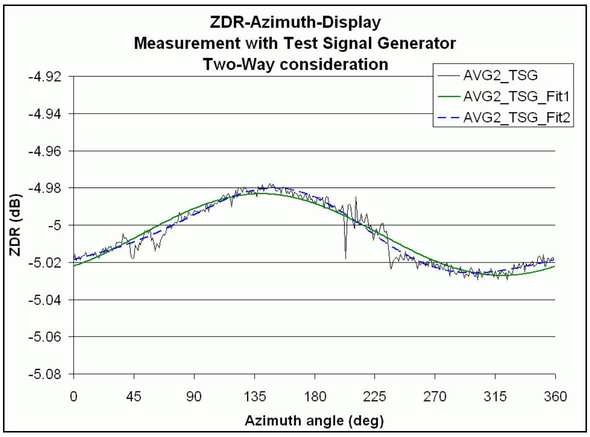

Figure 1: Two-way ZDR measurements with a test signal generator, as a function of antenna pointing azimuth angle. Average from 10 full turns is given (black), together with a first-order (green) and second-order (blue, dashed) Fourier fit.

---

* *Corresponding author address:*
Ronald Hannesen, Selex-Gematronik,
Raiffeisenstr. 10, 41470 Neuss, Germany;
e-mail: R.Hannesen@gematronik.com

2.2 Measurements in Stratiform Precipitation

During Jan and Feb 2007, several stratiform precipitation systems have been scanned. 360-deg ZDR-Azimuth displays were calculated based on the following rules:

- 10 range gates were radially averaged (at a range gate size of 0.2 or 0.25 km)
- At least 8 of these gates must have a signal 15 dB above noise level to form a valid ZDR-Azimuth pair
- The 360-deg ZDR-Azimuth display must be sufficiently stratiform and homogeneus, defined by:

$$N / Std_{ZDR} > 1600 \qquad (1)$$

where N is the number number of valid ZDR-aziumth pairs (max. 360), and Std_{ZDR} is the ZDR stddev (in dB) of all valid ZDR-aziumth pairs along a circle.

A total of 1677 ZDR-Azimuth displays were obtained. The cases were grouped for different elevation angles according to Table 1.

Table 1: Grouping of ZDR-Azimuth displays

Elevation angle interval	# cases
5 to 10 deg[(a)]	202
10 to 20 deg	348
20 to 60 deg	1039
60 to 90 deg	88
All	1677

[(a)] Elevation angles below 5 deg were omitted to avoid beam blocking influence

Figure 2 shows the averages for all 4 elevation angle groups. All patterns exhibit a sinusoidal curve, overlaid by random fluctuations. All sinusoidal curves have a similar phase and amplitude.

Figure 3 shows the average of all 1677 cases and a first-order and second-order Fourier fit. The phase of the first order fit is 139 deg, which is almost identical to the one obtained with the TSG measurements (section 2.1), and the variability is 0.061 dB, which is very similar to the TSG results. It is assumed that the ZDR-azimuth variability results from the Azimuth rotary joint. Since this variability is much smaller than the requested ZDR accuracy of 0.2 dB, it can be neglected for operational purposes.

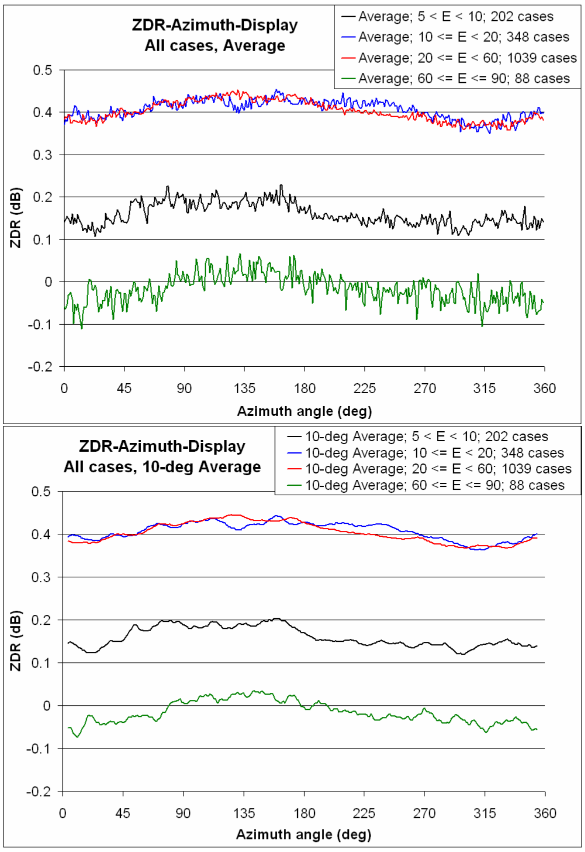

Figure 2: ZDR-Azimuth display; averages of several stratiform precipitation events. Top: data of single azimuths (rays). Bottom: 10deg running averages.

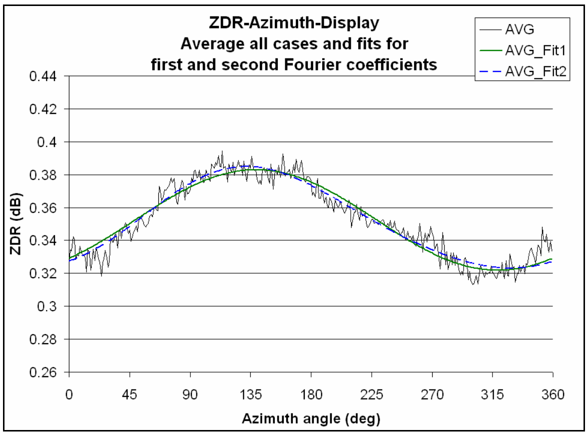

Figure 3: ZDR-Azimuth display; averages of several stratiform precipitation events (black); together with a first-order (green) and second-order (blue, dashed) Fourier fit.

2.3 Influence of the Wind Direction

The results of section 2 are averages of situations with different wind directions. In some cases, however, the amplitude of the sinusoidal curve was somewhat larger, in other cases smaller. Also, the phase was variable.

For that reason, the data were re-sampled. During re-sampling, first the second-order Fourier fit was subtracted from all data (as a result, an overall average as in Fig. 3 would no longer show any sinusoidal curve). Then, the ZDR-azimuth data were re-arranged in a way that the azimuth does not represent the geographic direction, but the direction relative to the wind direction at the radar site: 0 deg corresponds to where the wind blows from; then rotating clockwise.

When data then are averaged again similar to Fig. 2, a sinusoidal curve becomes evident again (Fig. 4). The variability of these curves is about 0.1 dB. The phase shows a different behaviour for cases with rain at the site than with snow at the site: In the former case, the phase is about 320 deg (i.e. the ZDR is highest shortly after the antenna turned “into the wind”), whereas for snowfall it is about 25 deg larger.

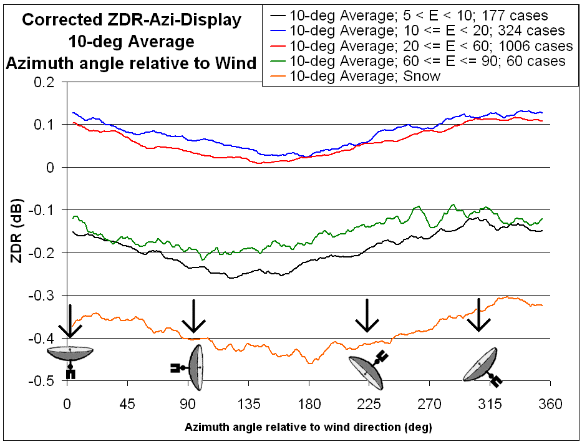

Figure 4: ZDR-Azimuth display (10 deg running averages), with azimuth being relative to the wind direction (arrows and antenna symbols represent antenna position relative to the wind).

Two reasons are possible for this wind-depending effect:

- The raindrops and snowflakes are aligned with the wind direction.
- The rain floating down the antenna dish causes differential attenuation, which depends on the antenna position relative to the wind (since “into the wind” it faces more rain than “away from the wind”). In case of snow, the melting time on the dish would cause some delay, which in turn would cause a clockwise phase shift (as observed) due to the clockwise antenna rotation.

It is not clear which of these effects really exist, and which one might be larger. Anyway, the variability is probably smaller than the ZDR accuracy needed for operational purposes.

3. BEAM BLOCKING EFFECTS

3.1 Theoretical Considerations

For sharp objects (such as large buildings, but also mountain ridges at large distances), the amount of beam blocking can be expected to be the same for the vertically polarized channel as for the horizontally polarized channel (provided that a proper horn feed is used, i.e. that the beam centers for both channels are identical). This means that ZDR data of partially blocked beams can be expected to be unbiased in such cases.

However, some obstacles might cause blocking or attenuation (or, more precisely, extinction) which depends significantly on the polarization, for example small metallic patterns at power lines. Also, trees may be the source of ZDR bias: for example, the small branches of deciduous trees, which are oriented rather vertically, in particular in the trees’ tops, would cause a stronger extinction of the vertically polarized radiation than of the horizontally polarized one, in particular in winter time when such trees are leafless. As a result, ZDR would be biased positively.

More generally, the amount of blocking can be expressed as an effective blocking angle Φ_S. (in deg, relative to the beam center). Then, the reflectivity loss can be expressed as (see Hannesen and Löffler-Mang, 1998; assuming a Gaussian intensity distribution and a homogeneous reflectivity factor in the resolution volume):

$$\Delta dBZ = 10 \log_{10}(\, 1 - \mathrm{erf}(\Phi_S/\Phi_0)\,) \qquad (2)$$

with $\Phi_0 = 0.43\,\eta_3$; η_3 being the 3dB beam width; and erf() being the integrated error function.

For obstacles with different effective blocking angles Φ_{SH} and Φ_{SV} for the horizontally and the vertically polarized radiation, respectively, the ZDR bias results as:

$$\Delta ZDR = \Delta dBZ_H - \Delta dBZ_V =$$

$$= 10 \log_{10}(1 - \mathrm{erf}(\Phi_{SH}/\Phi_0)) - 10 \log_{10}(1 - \mathrm{erf}(\Phi_{SV}/\Phi_0)) \quad (3)$$

Fig. 5 gives a systematic sketch of a situation where a positive ZDR bias would result from a forest with effective blocking angles $\Phi_{SH} < \Phi_{SV}$, i.e. where the vertically polarized radiation is blocked stronger.

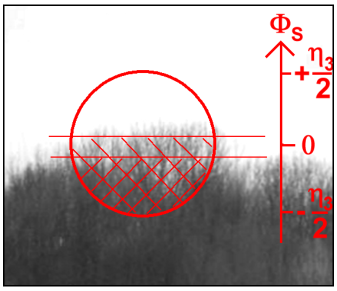

Figure 5: Sketch of a situation with $\Phi_{SH} < \Phi_{SV}$, i.e. larger blocking for the vertically polarized radiation.

In Fig. 6, the amount of ZDR bias is calculated from equation (3), assuming a 3dB beamwidth of $\eta_3 = 1$ deg. As can be obtained from that figure, even a small difference of the effective blocking angle causes a significant bias. The larger the blocking, the larger is also the ZDR bias, given a fixed blocking angle difference.

For example, if $\Phi_{SH} = 0.5$ deg, i.e. if the 3dB-part of the main lobe is just completely blocked, a difference of the effective blocking angles of only 0.1 deg causes a ZDR bias of more than 2 dB. In that case, the reflectivity bias due to blocking would be about –13 dB (Hannesen and Löffler-Mang, 1998, their Fig. 2).

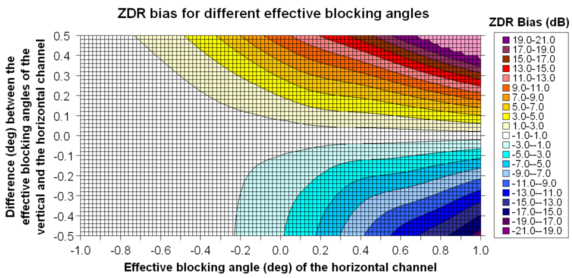

Figure 6: ZDR bias as a function of the effective blocking angles Φ_{SH} and Φ_{SV}. Note that on the ordinate, the difference $\Phi_{SV} - \Phi_{SH}$ is used.

3.2 Results

Fig. 7 shows a panoramic view around the Gematronik radar. Some trees, woods and buildings show top heights up to several degree elevation. Fig. 8 shows example PPIs at 1 deg elevation angle of reflectivity and ZDR. In several sectors, blocking is obvious from reduced reflectivity. Most sectors show increased ZDR indicating a positive ZDR bias from beam blocking.

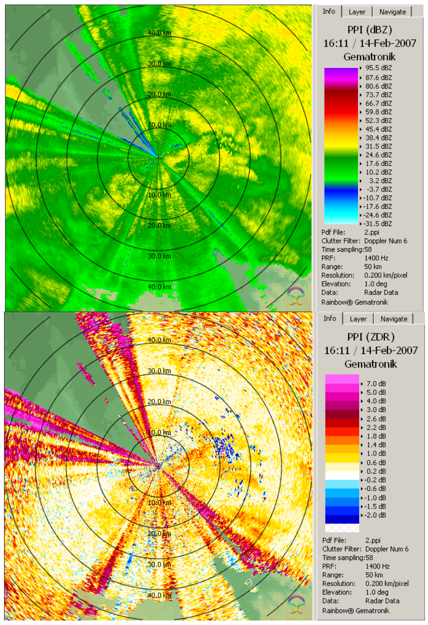

Figure 8: Example PPIs (1 deg elevation) of reflectivity (top) and differential reflectivity (bottom) of stratiform precipitation.

To investigate the blocking effects quantitatively, average reflectivity and ZDR profiles were calculated from PPI scans at 0.5, 1.0, 1.5, 2.0, and 3.0 deg elevation. Azimuth directions for different obstacles at different distances were used; for an overview see Table 2 and Fig. 9.

Table 2: Azimuth directions for vertical profiles

Azimuth	Obstacle	Distance	Top
43 deg	Hills with woods	~25 km	~0.5 deg
137 deg	Trees	~0.5 km	~2.0 deg
160 deg	Trees	~0.9 km	~1.0 deg
185 deg	Trees	~1.1 km	~1.0 deg
209 deg	Building	~0.1 km	~2.0 deg
218 deg	Building	~0.1 km	~0.5 deg
229 deg	Hills with woods	~12 km	~0.5 deg

Figure 7: Panoramic view around the Gematronik radar. Dashed lines (black-white) show 1 deg resolution. The horizontal lines are at 0 and +5 deg elevation, respectively.

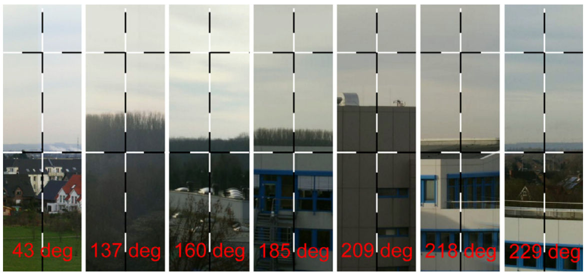

Figure 9: Sections of the panoramic view (Fig. 7) into the 7 azimuth directions of investigation (see Tab. 2).

Reflectivity and ZDR profiles were derived from several precipitation events in Jan and Feb 2007 (referred to as “winter”; deciduous trees leafless), and also during May 2007 (referred to as summer; deciduous trees with leaves). Ranges from behind the obstacles up to 50 km distance were used. Figure 10 shows several results of average profiles for the winter and the summer case. Also, fits to eqs. (2) and (3), respectively, are shown. The resulting effective blocking angles from the fits are given in Table 3 (with the blocking angles expressed relative to horizontal level).

Table 3: Effective blocking angles (deg), derived from vertical profile fits to eqs. (2) and (3)

Azimuth	Winter		Summer	
	Φ_{SH}	Φ_{SV}	Φ_{SH}	Φ_{SV}
43 deg	0.59	0.56	0.67	0.66
137 deg	1.69	1.80	2.17	2.16
160 deg	0.84	0.84	1.15	1.14
185 deg	1.20	1.21	1.52	1.52
209 deg	1.6	1.6	2.0	2.0
218 deg	0.6	0.6	0.8	0.8
229 deg	0.73	0.71	0.96	0.94

In Fig. 10, the difference between average reflectivity profile values and the corresponding fits is about 1 dB or less, even for reflectivity biases of more than 10 dB. This proves that eq. (2) properly represents the reflectivity bias from beam blocking, and that it can thus be used for beam blocking correction.

For ZDR, the vertical profiles show different characteristics for the different obstacles: For the building (at 218 deg azimuth) and for the far-distant hills with woods (43 deg), the ZDR profile is rather constant, proving that no ZDR bias occurs from such obstacles.

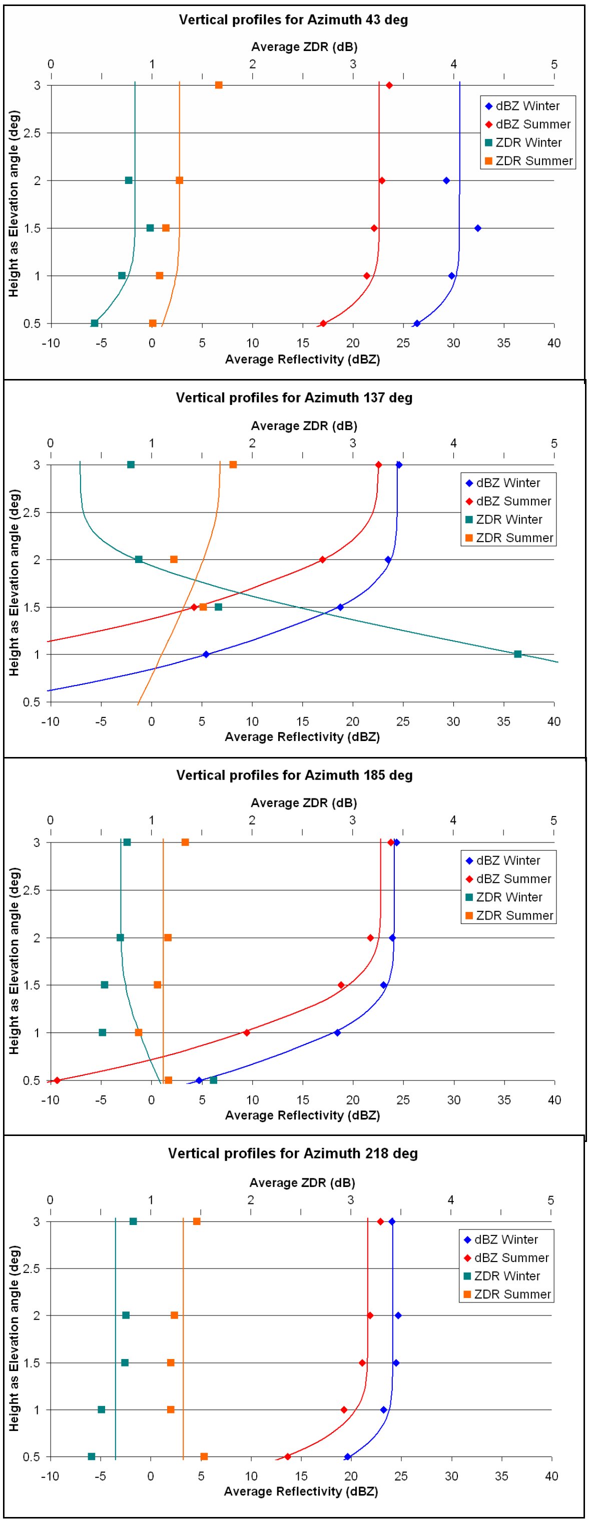

Figure 10: Average reflectivity and ZDR profiles for several azimuth directions. Fits to eqs. (2) and (3) are also shown.

For nearby deciduous trees (137 deg azimuth), a significant positive ZDR bias appears in winter, as can be expected from the many small vertical branches of such trees. In summer, this bias disappears, and the blocking angles are larger by about half a degree (see Table 3), due to the leaves causing much more blocking.

For deciduous trees at larger distance (185 deg azimuth), the above findings are much less pronounced: in winter, ZDR is biased at most about 1 dB (in cases of very high blocking); in summer the ZDR bias again vanishes.

In all cases the difference between the observed ZDR profiles and the corresponding fits is less than one dB, but typically several tenths of a dB. This means that a correction using eq. (3) would improve the data, but would often fail to reach the accuracy needed for operational measurements. Thus it may be necessary to extrapolate ZDR from upper elevations, in particular when the reflectivity is heavily biased.

4. SUMMARY AND CONCLUSIONS

In a first part, the azimuth dependence of ZDR was investigated using a test signal generator and long-time statistics of stratiform precipitation. The following conclusions are drawn:

- The systematic ZDR bias from the azimuth rotary joint is much smaller than the accuracy needed for operational measurements and thus can be neglected.
- For antennas without radome, a small systematic ZDR bias depending on the wind direction was observed, which may be due to wetting effects of the antenna dish. The variation of this bias is smaller than the accuracy needed for operational measurements.

In a second part, the influence of beam blocking on ZDR was investigated based on long-time observations of reflectivity and ZDR profiles in precipitation. The following conclusions are drawn:

- For objects with “sharp” boundaries, ZDR is unbiased.
- At small distances, trees can cause significant ZDR bias. This bias varies with season, in particular for deciduous trees.
- At large distances, forests appear as “sharp” objects.
- While reflectivity profiles might be corrected successfully using theoretical considerations, ZDR profile correction is more likely to fail to reach the accuracy needed for operational applications. Extrapolation of ZDR from upper elevations might be necessary.

5. REFERENCES

Bringi, V.N., T.D. Keenan and V. Chandrasekar (2001): Correcting C-band radar reflectivity and differential reflectivity data for rain attenuation: A self-consistent method with constraints. *IEEE Trans. Geosci. Remote Sens.*, **39**, 1906-1915.

Hannesen, R., and M. Löffler-Mang (1998): Improvement of quantitative rain measurements with a C-band Doppler radar through consideration of orographically induced partial beam screening. *Proc. COST 75 Seminar, Switzerland, 23-27 March 1998 (European Commission EUR 18567 EN)*, 511-519.

Giangrande, S.E., and A.V. Ryzhkov (2005): Calibration of dual-polarization radar in the presence of partial beam blockage. *J. Atmos. Ocean. Technol.,* **22**, 1156-1166.

Gourley, J.J., P. Tabary, and J. Parent du Chatelet (2006): Data Quality of the Meteo-France C-band polarimetric radar. *J. Atmos. Ocean. Technol.,* **23**, 1340-1356.

Manz, A., T. Monk, and J. Sangiolo (1998): Radome effects on weather radar systems. *Proc. COST 75 Seminar, Switzerland, 23-27 March 1998 (European Commission EUR 18567 EN)*, 467-477.

Melnikov, V.M., D.S. Zrnić, R.J. Doviak, and J.K. Carter (2003): Calibration and performance analysis of NSSL’s polarimetric WSR-88D. *NSSL report*, 72pp.